Time-resolved isothermal crystallization of absorbable PGA-*co*-PLA copolymer by synchrotron small-angle X-ray scattering and wide-angle X-ray diffraction

Zhi-Gang Wang[a], Xuehui Wang[a], Benjamin S. Hsiao[a,*], Saša Andjelić[b], Dennis Jamiolkowski[b], James McDivitt[b], Jerome Fischer[b], Jack Zhou[b], Charles C. Han[c]

[a]*Department of Chemistry, State University of New York at Stony Brook, Stony Brook, NY 11794-3400, USA*
[b]*Ethicon, Inc., a Johnson and Johnson Company, P.O. Box 151, Somerville, NJ 08876-0151, USA*
[c]*Polymers Division and Center for Neutron Research, National Institute of Standards and Technology, Gaithersburg, MD 20899, USA*

This work is devoted to Prof. Stein on the occasion of his 75th birthday

Abstract

The isothermal crystallization behavior of absorbable dyed and undyed PGA-*co*-PLA copolymers was investigated by time-resolved simultaneous small-angle X-ray scattering (SAXS) and wide-angle X-ray diffraction (WAXD) methods with synchrotron radiation. The morphological parameters extracted from time-resolved SAXS profiles show that long period and lamellar thickness decrease slightly after primary crystallization. The unit cell parameters a and b and the apparent lateral crystal sizes L_{110} and L_{020} were extracted from the corresponding WAXD profiles. A significant decrease in the unit cell parameters and a substantial increase in the apparent crystal sizes are seen during the initial crystallization stage. Both scattering invariant (Q from SAXS) and crystallinity (X_c from WAXD) results indicate that the crystallization rate is the fastest at 130°C. These copolymers show a bell-shape crystallization rate curve with temperature, where the dyed copolymer has a faster crystallization rate than the undyed one even though the inclusion of the low molecular weight organic dye is very small (ca. 0.2% by weight). We conclude that the dye molecule, which enhances the visibility during surgery, acts as a nucleating agent that increases the overall crystallization rate. The crystallization rate at 90°C is significantly slower than that at 130°C, however, the long period and lamellar thickness formed at 90°C are much lower than those formed at higher temperatures. The dyed and undyed PGA-*co*-PLA copolymers have almost the same morphological parameters at the same temperature. This indicates that morphological parameters of the lamellar structures in the polymers depend primarily on the crystallization temperature rather than on the crystallization rate. It is evident that the thermodynamic factor driven by temperature principally determines the lamellar morphology. The final unit cell parameters a and b and the final apparent crystal sizes all increase with temperature, indicating that crystal perfection prevails at high temperatures. © 2001 Elsevier Science Ltd. All rights reserved.

Keywords: PGA-*co*-PLA; Absorbable polymer; Lamellar

1. Introduction

Polyglycolide (PGA), polylactide (PLA) homopolymers and PGA-*co*-PLA copolymers are linear aliphatic polyesters, all known as biodegradable or absorbable polymers, with properties suitable for biomedical applications in medical devices such as sutures, orthopedic implants and controlled release carriers for drugs [1–3]. Most of the existing studies on these polymers are concerned with their preparation schemes and the corresponding degra-

dation behaviors [4–15]. For example, the degradation behavior in PGA-*co*-PLA copolymers in the aqueous media has been widely investigated as functions of time, temperature, crystallinity, and the pH level on properties such as molecular weight composition and mechanical strength [5–15]. At a constant composition, the rate of degradation has been found to be a function of the crystallinity as well as morphological feature. It has been proposed that the degradation process proceeds through two separate stages with different rates, which correlates with the amorphous and crystalline regions in the sample [9,10]. Hydrolytic attack is first initiated in the amorphous region [11]. In several selected crystalline systems, it has been
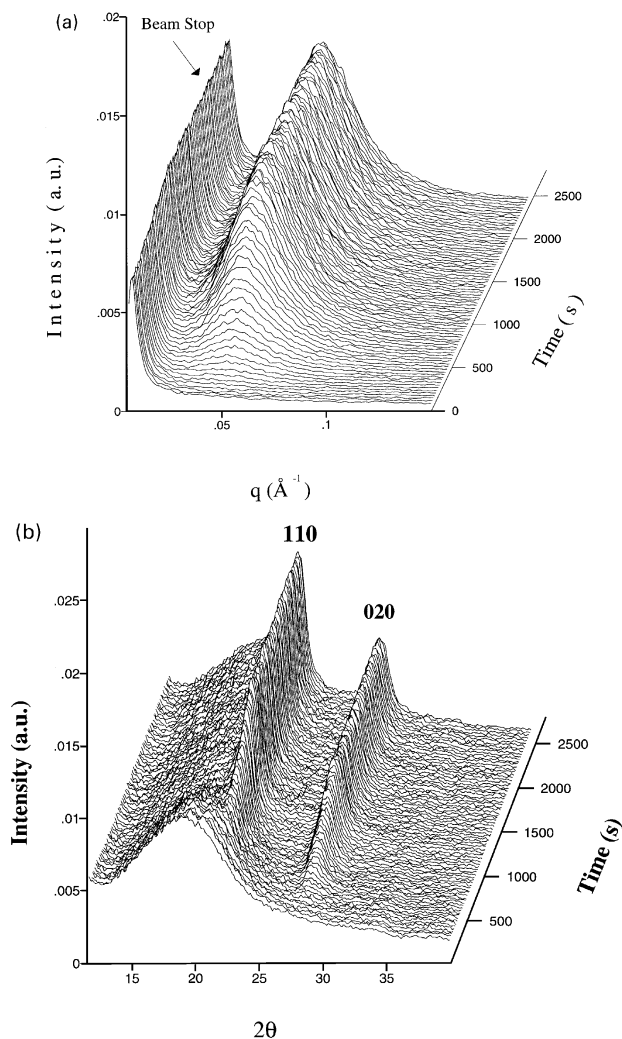
Fig. 1. Time-resolved (a) SAXS and (b) WAXD 3-dimensional profiles of dyed PGA-*co*-PLA copolymer during isothermal crystallization at 130°C.

confirmed that morphological variables at the lamella level also play an important role in the degradation mechanism [16–18].

The aim of this work is to study the time-resolved isothermal crystallization behavior and the corresponding changes in structure and morphology of PGA-*co*-PLA copolymers at both lamellar (10–1000 Å) and unit cell (1–10 Å) levels using simultaneous small-angle X-ray scattering (SAXS) and wide-angle X-ray diffraction (WAXD) techniques with synchrotron radiation. The chosen isothermal crystallization temperatures covered a wide range of temperature, during which a bell-shaped crystallization rate curve was observed. This wide temperature range is very different from our previous work on a similar PGA-*co*-PLA copolymer system, where only a few selected temperatures were used [17]. The degree of crystallinity, crystal sizes and unit cell parameters (*a* and *b*) have been obtained from the WAXD analysis, and the lamellar morphological variables such as long period, lamellar thickness, and amorphous layer thickness have been determined by SAXS analysis. Finally, as surgical sutures are frequently dyed to facilitate the visualization in the surgical site, the influence of the dye molecules (at approximately 0.2% by weight) on the crystallization behavior and morphological structure of PGA-*co*-PLA copolymers is also investigated.

2. Experimental

2.1. Materials and preparation

The polymers used in this study were dyed and undyed PGA-*co*-PLA copolymers, supplied by Ethicon Inc. These samples were random copolymers containing 90% (by weight) glycolide and 10% L-lactide (90/10 PGA-*co*-PLA) and had an intrinsic viscosity of 1.58 dL/g (as measured in hexafluoro-2-propanol at 25°C at a concentration of 0.1 g/dL). The resins had a weight average molecular weight (M_w) of approximately 75,000 g/mol and a number average molecular weight (M_n) of approximately 24,000 g/mol as determined by GPC.[1] The polydispersity (M_w/M_n) was 3.125. The intrinsic viscosity of the died sample was 1.56 dL/g. The nominal melting temperature was 201°C, measured by DSC using a heating rate of 20°C/min. The dye compound was D and C Violet No.2, 1-hydroxy-4-[(4-methylphenyl)-amino]-9,10-anthracenedione, added at approximately 0.2% by weight. Surgical sutures are frequently dyed to aid in their visualization in the surgical site. Polymer films were prepared using an MTP-14 Tetrahedron™ compression molding press operated under a high flow of nitrogen. The raw pellets were melted in a mold frame at 225°C for 5 min and 1.0×10^8 Pa pressure for 3 s to produce uniform films with the following dimension: $15.2 \times 15.2 \times 0.10$ cm. Processing induced degradation was minimal [18]. Due to the high sensitivity of the polymer to hydrolytic degradation, the samples were stored under vacuum. Prior to the SAXS measurement, the samples were retrieved from vacuum storage and cut into 7 mm diameter discs.

2.2. SAXS/WAXD measurements

Simultaneous SAXS and WAXD measurements were carried out at the Advanced Polymers Beamline, X27C, National Synchrotron Light Source (NSLS), Brookhaven National Laboratories (BNL). The wavelength of the X-ray beam was 1.307 Å with a beam size about 0.4 mm in diameter at the sample position. Synchrotron X-rays were collimated using a three 2° tapered tantalum pinhole collimator [19]. The SAXS/WAXD profiles were collected by the two position
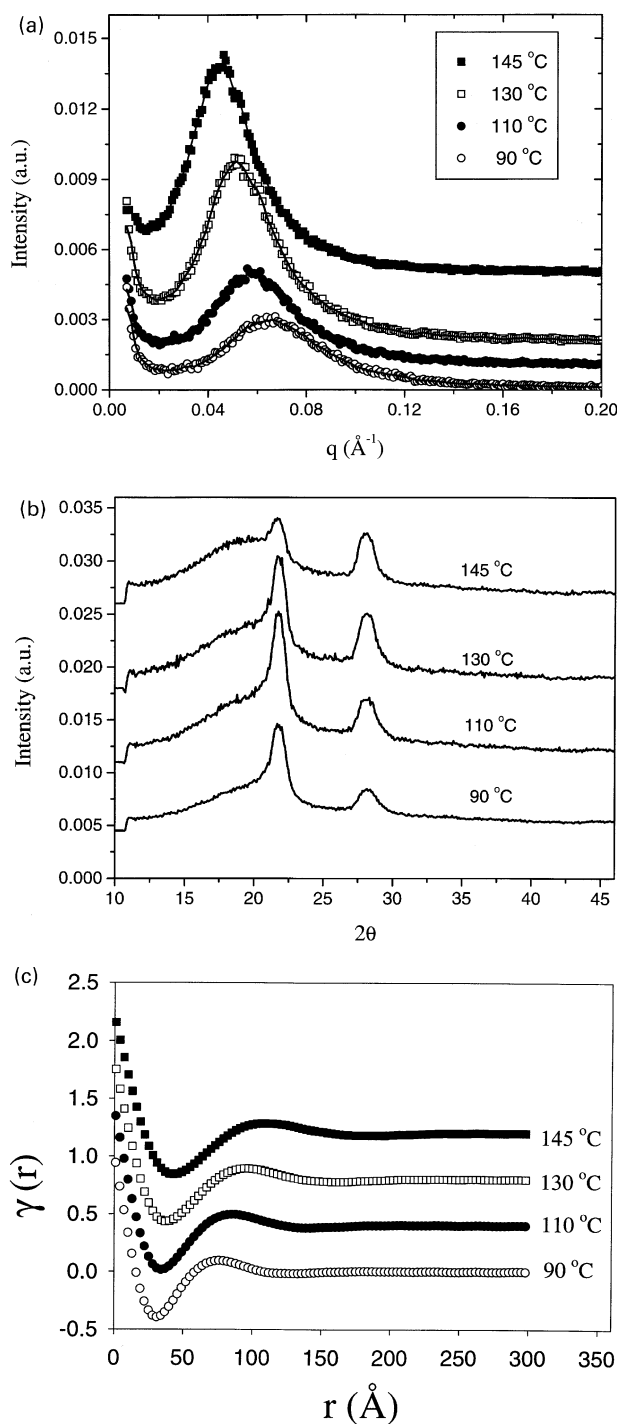
Fig. 2. The final profiles of (a) SAXS, (b) WAXD, and (c) the corresponding correlation functions at different temperatures for dyed PGA-*co*-PLA copolymer and the peak deconvolution of one WAXD profile.

sensitive detectors (from European Molecular Biological Laboratory, EMBL) with sample-to-detector distances of 1830 mm for SAXS and 110 mm for WAXD, respectively. The SAXS angle was calibrated with silver behenate and the intensity was normalized for incident beam fluctuations. The WAXD pixel resolution and the intensity were calibrated by comparing the synchrotron data with the

Siemens Hi-Star X-ray diffractometer data (CuKα) in $\theta-\theta$ reflection, and were corrected for detector non-linearity and the empty beam scattering. The angular scale of the synchrotron WAXD data ($\lambda = 1.307$ Å) was also converted to a scale corresponding to $\lambda = 1.542$ Å for presentation and discussion.[2]

A dual chamber temperature jump apparatus was used for the isothermal crystallization studies. A detailed description of the setup has been reported elsewhere [20]. In this study the samples were first melted at 230°C (30°C above the nominal melting point of PGA-*co*-PLA) for 7 min in one chamber and then pneumatically 'jumped' to the second chamber. This second chamber was preheated at the desired crystallization temperature, aligned in the path of the X-ray beam. Isothermal crystallization runs were conducted at 90, 110, 130 and 145°C for dyed copolymer, and 110 and 130°C for undyed copolymer. The estimated time for temperature equilibration after the jump was about 60 s. The temperature fluctuation is ±0.5°C. The collection time for each simultaneous SAXS/WAXD frame was 30 s.

3. Results and discussion

Fig. 1 shows typical time-resolved (a) SAXS and (b) WAXD profiles, developed during isothermal crystallization at 130°C for the dyed PGA-*co*-PLA sample. During the isothermal crystallization period, initial SAXS profiles show a sharp monotonic decrease in the intensity near the beam-stop position, which is related to a completely disordered structure in the supercooled melt. The scattered intensity profile first exhibits a small maximum at ca. $q = 0.052$ Å^{-1} at 20 s, which subsequently increases significantly until reaching a plateau value. There is no distinct increase of the low-angle intensity near the beam-stop position. The SAXS peak can be attributed to the lamellar structure in the spherulites of PGA-*co*-PLA copolymer, which has been discussed before [21]. The initial isothermal WAXD profiles show only one amorphous halo, on which the evolution of an orthorhombic unit cell structure of the PGA crystal can be followed by the corresponding {110} and {020} reflections marked in Fig. 1b [22]. The intensities of the crystal reflections {110} and {020} increase notably during early stages of crystallization and remain almost constant during the late stages of crystallization. The increases in the WAXD reflections have almost the same rate as that in SAXS scattering invariant at 130°C. The unit cell for the PGA crystal is orthorhombic, having $a = 5.25$ Å, $b = 6.19$ Å, and $c = 7.02$ Å, which will be used as a reference for calculation of cell parameters [22].

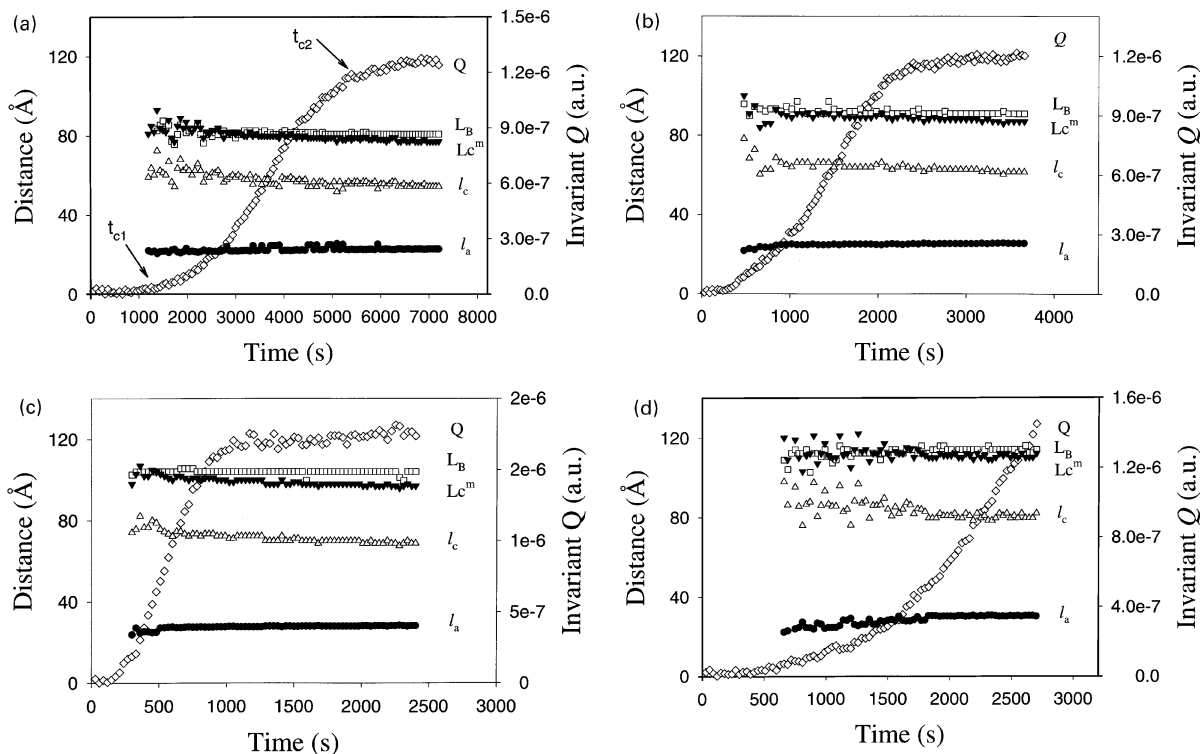Fig. 2a shows the final experimental SAXS profiles

Fig. 3. Time evolution of Bragg spacing, L_B, long period from correlation function, L_c^m, crystal thickness, l_c, amorphous thickness, l_a, and the scattering invariant, Q, during isothermal crystallization for dyed PGA-*co*-PLA copolymer at different temperatures (a: 90°C; b: 110°C; c: 130°C; d: 145°C). Note that the relative standard deviation for L_B (and L_c^m, l_c, l_a) and Q (and X_c in Fig. 7) are less than 1% and 2%, respectively.

collected at different temperatures for dyed PGA-*co*-PLA copolymer. It can be seen that the SAXS peak shifts to lower q positions at higher isothermal crystallization temperatures, indicating the larger long spacings in the lamellar stacks. For time-resolved SAXS profiles, the procedures for calculating morphological parameters in the semi-crystalline polymers have been extensively discussed in earlier publications [23–25]. These procedures involve the use of correlation functions (shown in Fig. 2c, which were calculated from the data in Fig. 2a) and interference distribution functions to extract parameters such as scattering invariant (Q), long spacing (L) and the thicknesses of the constituting two phases (crystal and amorphous thicknesses, l_c and l_a). For this study, we choose to assign the large value l_1 calculated from the correlation function as the crystal thickness, l_c, and the small value l_2 as the amorphous thickness, l_a. Our reasons have been given before [17,25–28] and will not be given again in this paper.

Fig. 2b shows the final experimental WAXD profiles of dyed PGA-*co*-PLA measured at different temperatures. From these WAXD profiles, the peak position, peak height, peak width and integrated intensity, for each crystal reflection and amorphous background can be obtained by using a custom code capable of dealing with time-resolved spectra. Two Gaussian peaks riding on a baseline is used to fit the amorphous background, and all other crystal reflection peaks are also fitted with Gaussian functions. By dividing the total intensities of the crystalline reflections I_c with the

overall intensity I_{total}, a measure of the mass fraction of the crystalline phase (X_c) in the sample can be obtained. Because of the possible defects in the crystal lattice and thermal disordering, the measured value of I_c should be lower than the true value. We note that by using this deconvolution method, the sample is assumed to possess two ideal phases (crystalline and amorphous), which is the criterion to define the term 'crystallinity' [29]. Since the crystal reflection signals are extremely weak in the early stages of crystallization, the determination of the crystallinity is stopped when the crystal reflection {110} cannot be isolated. From the peak positions and peak widths of {110} and {020} of the crystalline WAXD profiles, the unit cell parameters of a and b (orthorhombic unit cell) and the apparent lateral crystal sizes L_{110} and L_{020} can be calculated [29]. The apparent lateral crystal sizes are deduced from the Scherrer equation: $L_{hkl} = K\lambda/(\beta\cos\theta)$, where the shape factor K is set equal to 0.9 as for most polymer systems, λ is the wavelength used, β is the half width (in radians) of the crystal reflection, and 2θ is the position of the (hkl) reflections.

Fig. 3 summarizes the time evolution of the morphological parameters extracted from the SAXS profiles during isothermal crystallization of dyed PGA-*co*-PLA at different temperatures (Fig. 3a–d) and for undyed PGA-*co*-PLA copolymer at 130°C (not shown here as its general behavior is very similar to that of the dyed sample). The morphological parameters shown include the Bragg spacing, L_B; long period from correlation function, L_c^m; crystal thickness, l_c;
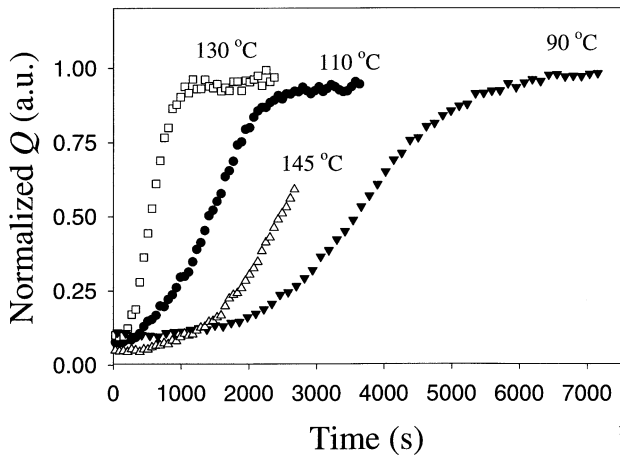
Fig. 4. Time evolution of normalized SAXS scattering invariant Q at different temperatures for dyed PGA-co-PLA copolymer.

Fig. 6. The final SAXS Bragg spacing, L_B^*, long period from correlation function, L_c^{m*}, crystal thickness, l_c^*, and amorphous thickness, l_a^*, at different temperatures for both dyed and undyed PGA-co-PLA copolymers.

amorphous thickness, l_a; and the scattering invariant, Q. The common characterization in Fig. 3a–d can be found as follows: (1) the primary isothermal crystallization period can be defined during the time period $t_{c1} < t < t_{c2}$ (arrow-marked in Fig. 3a) [25]. In this period, the SAXS profiles start to show a peak, which grows continuously at a rapid rate. The morphological parameters of Bragg spacing (L_B), long period (L_c^m), crystal thickness (l_c) and amorphous thickness (l_a) at the later times in this stage appear to reach stable values as those in the secondary crystallization stage, defined by the time when $t > t_{c2}$. We note that t_{c1} and t_{c2} may correspond to the onset of the spherulitic growth and the point of spherulitic impingement, respectively. However, this assertion needs to be further verified by optical microscopy. Interestingly, the values of long period (L_c^m) and crystal thickness (l_c) during early times all show a noticeable decrease. (2) During the secondary crystallization stage (when $t > t_{c2}$), long period (L_c^m) and crystal thickness (l_c) also show a small but definite decrease with time. (3) The amorphous thickness, l_a, shows a slight increase

during the primary crystallization stage and is almost constant during the secondary crystallization stage.

For the clear comparison of the differences in Fig. 3a–e, Figs. 4–6 are plotted. Fig. 4 displays the invariant Q with time at different temperatures for dyed PGA-co-PLA copolymer. An Avrami-like behavior is seen during the primary crystallization stage, while a slight increasing Q value is seen during the secondary crystallization stage. Of the four temperatures studied, it is interesting to find that the crystallization rate is the slowest at the lowest isothermal crystallization temperature of 90°C. The maximum crystallization rate for this sample was observed at the crystallization temperature of 130°C. The reciprocal values of the characterization times t_{c1} and t_{c2}, which indirectly represent the crystallization rates (we note that the crystallization half time is located between t_{c1} and t_{c2}), are plotted in Fig. 5. The fastest primary crystallization rate (or the shortest time) is found at $T_c = 130$°C. A similar result has
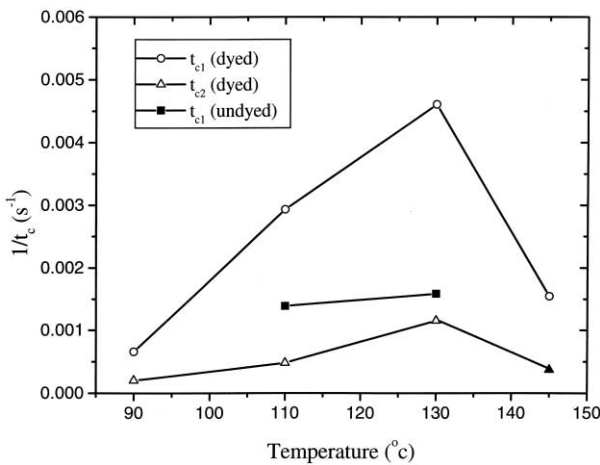

Fig. 5. The reciprocal characteristic time of primary crystallization at different temperatures for dyed and undyed PGA-co-PLA copolymers.
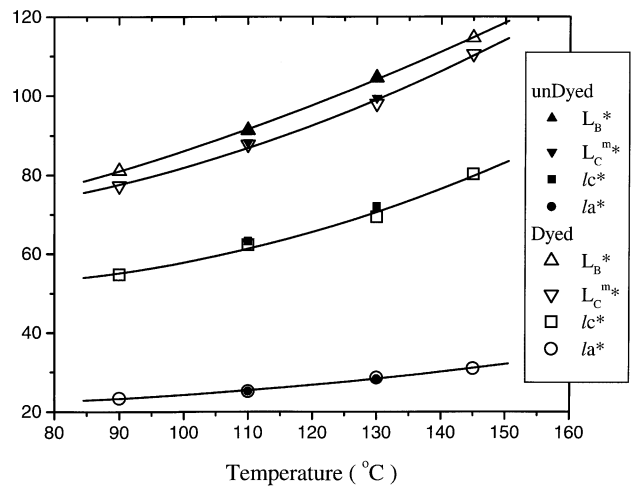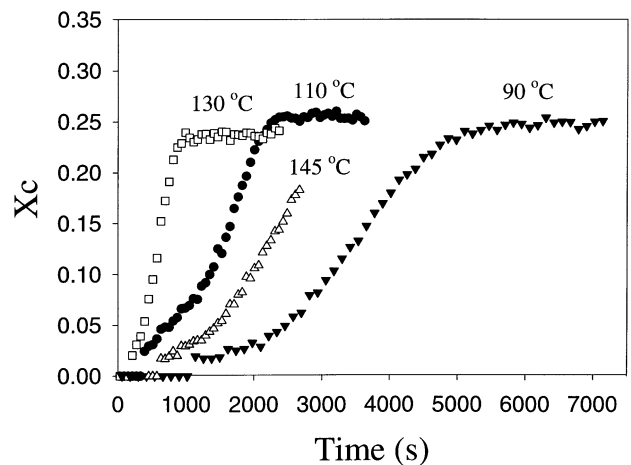

Fig. 7. Time evolution of WAXD crystallinity, X_c, at different temperatures for dyed PGA-co-PLA copolymer.
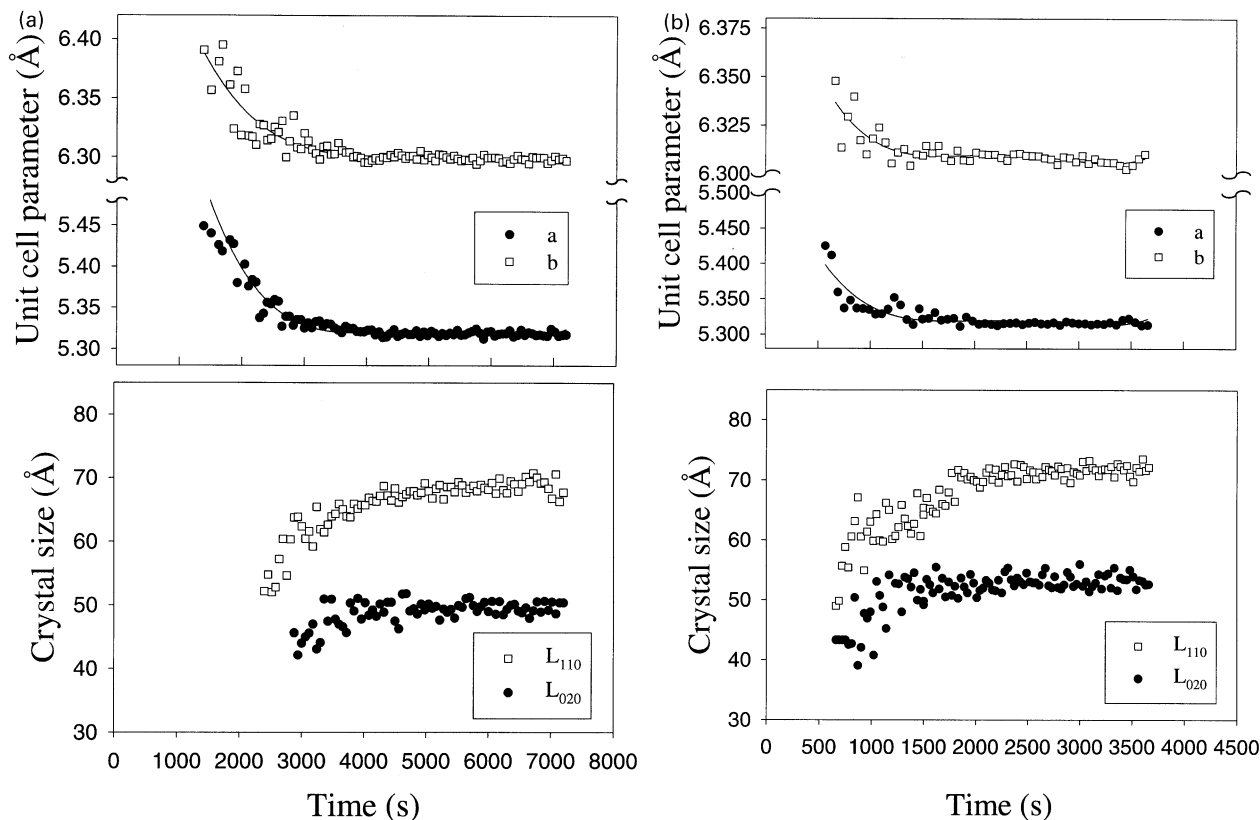
Fig. 8. Time evolution of the unit cell parameters, *a* and *b*, (top); and apparent crystal sizes, L_{110} and L_{020}, during isothermal crystallization for dyed PGA-co-PLA copolymer at different temperatures (a: 90°C; b: 110°C; c: 130°C; d: 145°C). Note that the relative standard deviation for *a*(and *b*) and L_{200} (and L_{020}) are less than 1 and 2%, respectively.

been reported in dyed PGA-*co*-PLA copolymer using a different technology before [21]. Fig. 5 can be directly related to the curve of bulk crystallization rate with temperature, which shows a bell-shape. Such a shape in crystallization rate is usually attributed to the growth process (the secondary nucleation process is the dominating step at high temperatures, and the transport process is the dominating step at low temperatures). Compared with the dyed PGA-*co*-PLA copolymer, the undyed copolymer has a longer crystallization characterization time of t_{c1}, indicating a slower nucleation rate. It is noted that t_{c2} for undyed PGA-*co*-PLA copolymer was not detected due to its relatively longer crystallization time and a limited available synchrotron beam time during measurements. However, there is no doubt that the dye in the absorbable polymer increases the overall crystallization rate. Even though its content is small (only 0.2% by weight), the addition of dye shows a significant influence on the crystallization rate of PGA-*co*-PLA. It is reasonable to conclude that the dye molecules serve as an effective heterogeneous nucleating agent for this sample.

Fig. 6 summarizes the final Bragg spacing, L_B^*, long period, L_c^{m*}, lamellar thickness, l_c^*, and amorphous thickness, l_a^*, of dyed and undyed PGA-*co*-PLA copolymers after isothermal crystallization. It can be seen that L_B^*, L_c^{m*}, and

l_c^* exhibit a clear increase with crystallization temperature T_c while l_a^* only shows a slight increase with T_c. This phenomenon has been observed in other semi-crystalline polymers before, such as PBT [25], PET [26], Nylon 66 [27] and PP [29]. Compared with the in-situ X-ray studies mentioned earlier, the major feature in this work and our recently reported [30] work on another absorbable biopolymer, poly(*p*-dioxanone), lies on the isothermal crystallization temperature range used. In this work and in Ref. [30], the chosen temperature range covers both sides of the bell-shape crystallization kinetics curve. The previous studies performed on non-absorbable polymers have just employed the temperature range on the right side of the crystallization rate curve, which is in the nucleation-controlled region. Usually, the nucleation process is so fast at the lower crystallization temperatures (the left side of the crystallization rate curve) that time-resolved X-ray methods cannot follow the early stages of crystallization. For this PGA-*co*-PLA copolymer, the relatively slow crystallization rate at lower temperatures makes it possible to study the formation of lamellae in the growth-controlled region. Even with the slow crystallization rate at 90°C, the lamellar thickness formed at this T_c is still the smallest one among those produced at other temperatures. Larger lamellar thickness and larger long period are always formed at higher
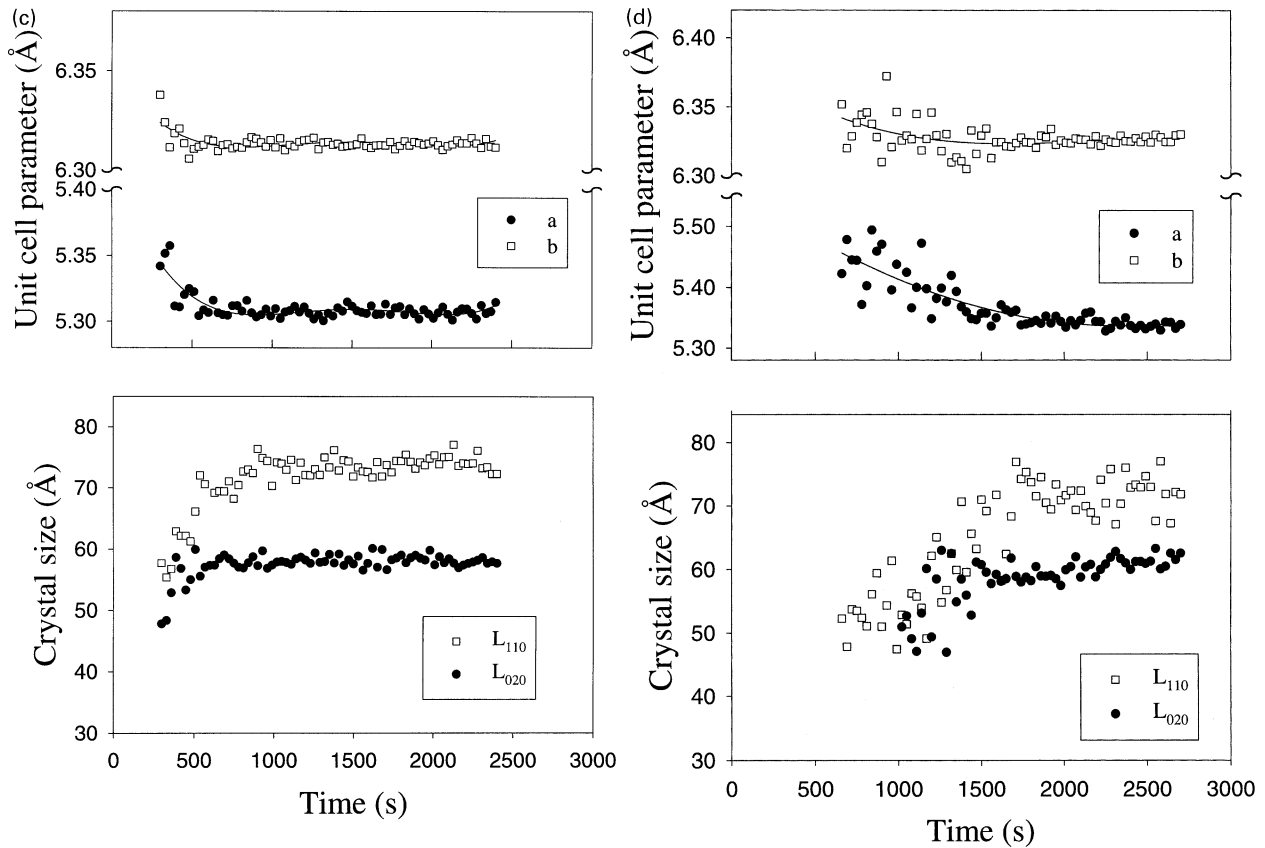
Fig. 8. (*continued*)

temperatures, which can be explained by the higher chain segmental mobility. The higher chain mobility results in a higher possibility for polymer chain segments to disentangle, diffuse and reorganize into larger chain-folding lamellae. Increase in lamellar thickness with increasing T_c was also observed for poly(p-dioxanone) homopolymer and its copolymers [30].

Fig. 7 displays the WAXD crystallinity (X_c) with time at different temperatures for dyed PGA-*co*-PLA copolymer. The time evolution of crystallinity profile, very similar to the time evolution of the SAXS invariant (Q) profile, also shows an Avrami-like growth behavior during the primary crystallization stage. Later, a constant value of X_c is seen during the secondary crystallization stage of all the chosen temperatures. The same crystallization kinetics curve can be obtained from the X_c profiles at different temperatures.

Fig. 8 summarizes the changes of structural parameters (orthorhombic unit cell parameters a and b; lateral crystal sizes, L_{110} and L_{020}), extracted from the WAXD data during isothermal crystallization of dyed PGA-*co*-PLA at different temperatures (a–d). Because of the weak reflection signals in WAXD during the very early stage of primary crystallization, the unit cell parameters and the crystal sizes at this stage are not accessible. It is seen that the unit cell parameters a and b show a distinct decrease with time at all temperatures during primary crystallization. The changes

of the unit cell parameters with time have been fitted by a fourth order polynomial equation ($Y = B_0 + B_1 t + B_2 t^2 + B_3 t^3 + B_4 t^4$), where Y represents the unit cell parameters, and t represents the time. The coefficient B_1 can be used to approximate the rate of decrease in the unit cell parameter, as shown in Fig. 9. It is interesting to see that a more significant decrease takes place at lower temperatures. This may be caused by the relatively more defective crystals formed at
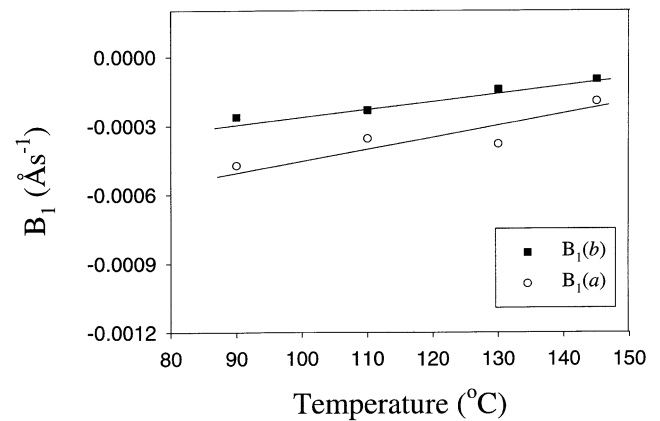

Fig. 9. The coefficient B_1 (the rate of the unit cell parameter decreases) at different temperatures for dyed PGA-*co*-PLA copolymer.
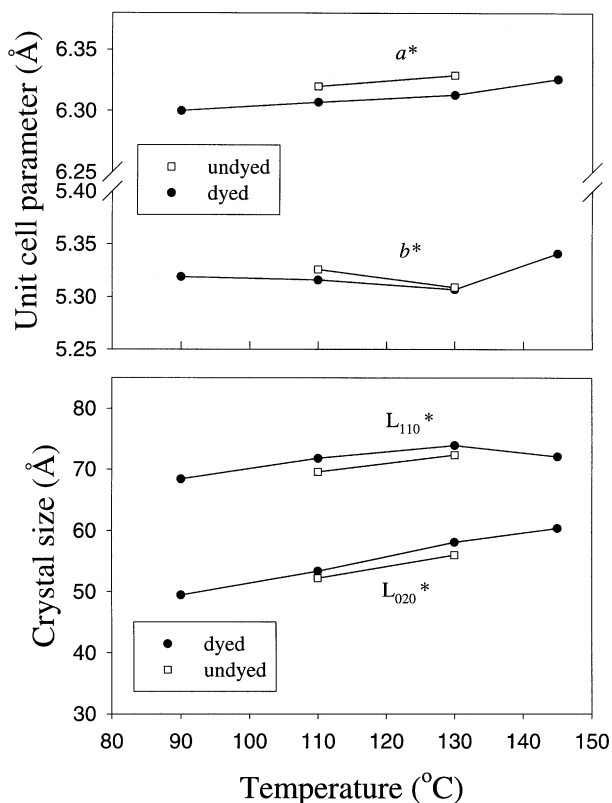
Fig. 10. The final unit cell parameters, a^* and b^*, (top); and apparent crystal sizes, L_{110}^* and L_{020}^*, at different temperatures for both dyed and undyed PGA-co-PLA copolymers.

lower temperatures, which have a better possibility for perfection. The contraction of the unit cell parameters during isothermal crystallization has been observed in other polymers and has been attributed to polymer crystal perfection [31–34]. Another interesting observation is that during secondary crystallization, the unit cell parameters are about constant, but the apparent lateral crystal sizes L_{110} and L_{020} show a small but noticeable increase (the increase of L_{110} is more than that of L_{020}) with time at all temperatures. During primary crystallization, the size increases are significant. These results indicate a larger lateral crystal growth along the a direction than that along the b direction. A similar phenomenon has also been reported on the annealing of quenched isotactic polypropylene, where a rapid increase in apparent crystal sizes of L_{110} and L_{040} was observed during primary crystallization [35]. The final unit cell parameters and the final apparent crystal sizes obtained at different crystallization temperatures are shown in Fig. 10. A slight increase of the unit cell parameter a^* with temperature is observed, while unit cell parameter b^* shows only a larger value at 145°C. Dyed PGA-co-PLA copolymer shows lower values of the unit cell parameters when compared to those of undyed PGA-co-PLA. The final crystal sizes L_{110}^* and L_{020}^* are also found to increase with crystallization temperature, which is consistent with the results obtained

on isotactic polypropylene crystallized from melt state [35]. Dyed PGA-co-PLA copolymer produces a larger crystal than undyed copolymer at the same isothermal crystallization temperature. At the same temperature, the influence of dye on the unit cell dimensions and crystal sizes can be explained by its effect on the crystallization rate. The faster crystallization rate produces smaller unit cell and larger crystal sizes because of longer crystallization time for crystal perfection (unit cell contraction) and growth. However, the temperature-dependent crystallization rate does not show this effect clearly, for example, a^* is not the lowest value at 130°C and L_{020}^* is not lower than that at 130°C. This is probably due to the different isothermal crystallization time used in the measurements.

4. Conclusions

Time-resolved simultaneous synchrotron SAXS and WAXD method was used to study isothermal crystallization in bio-absorbable dyed and undyed PGA-co-PLA copolymers. The lamellar morphological parameters such as long period and lamellar thickness extracted from time-resolved SAXS profiles showed obvious decreases in the very early stages during primary crystallization, which can be explained by the lamellar stack insertion process. Time-resolved WAXD profiles were deconvoluted to show that the unit cell parameters a and b exhibited significant decreases and the apparent lateral crystal sizes L_{110} and L_{020} showed significant increases during primary crystallization stage. These parameters, however, were almost constant during the secondary crystallization stage. The time evolution profiles of the scattering invariant, Q, (SAXS) and the crystallinity (WAXD) demonstrated that crystallization was fastest near 130°C. The reciprocal values of the characteristic time, t_c, illustrated that these copolymers showed a bell-shape crystallization rate and that dyed PGA-co-PLA had a faster crystallization rate than the undyed material even though the content of the dye was very small (0.2% by weight). The purple dye, which makes the suture materials more visible during surgery, is an effective nucleating agent to increase the bulk crystallization rate of PGA-co-PLA (this was also confirmed by the increase in nucleation density under polarized optical microscope). Even though the crystallization rate is much slower at 90°C than that at higher temperatures (110, 130 and 145°C), the final long period and the lamellar thickness formed at 90°C are still lower than those formed at higher temperatures. In addition, although they exhibit very different crystallization rates, the dyed and undyed PGA-co-PLA copolymers have almost the same lamellar morphological parameters at the same temperature. This confirms that the morphological parameters in these polymers depend only on the crystallization temperature. The final unit cell parameters a and b, and the final apparent crystal sizes, however, were found to increase with temperature.

Acknowledgements

References

[1] Zhang X, Goosen FA, Wyss UP, Pichor D. Rev Macromol Chem Phys 1993;C33:81.
[2] Herrmann JB, Kelly RJ, Higgins GA. Arch Surg 1970;486:100.
[3] Chu CC. The biomedical engineering handbook. CRC Press, 1995. (p. 611).
[4] Gilding DK, Reed AM. Polymer 1979;1459:20.
[5] Reed AM, Gilding DK. Polymer 1981;22:494.
[6] Gopferich A. Biomaterials 1996;103:17.
[7] Miller ND, Williams DF. Biomaterials 1984;365:5.
[8] Pistner H, Bendix DR, Muhling J, Reuther JF. J Biomater 1993;291:14.
[9] Chu CC. J Biomed Mater Res 1981;15:19.
[10] Chu CC. J Appl Polym Sci 1981;26:1727.
[11] Fredericks RJ, Melveger AJ, Dolegiewitz LJ. J Polym Sci, Polym Phys 1984;57:22.
[12] Cohn D, Younes H, Maron G. Polymer 2018(1987):28.
[13] Vert M, Mauduit J, Li S. Biomaterials 1994;119:15.
[14] Vert M, Li SM, Garreau H. J Biomater Sci, Polym Ed 1994;639:6.
[15] Vert M, Li SM, Garreau H. J Controlled Release 1991;15:16.
[16] King E, Cameron RE. J Appl Polym Sci 1997;66:1681.
[17] Wang ZG, Hsiao BS, Zong SXH, Zhou J, Dormier E, Jamiolkowski DD. Polymer 2000;41:621.
[18] Zong XH, Wang ZG, Hsiao BS, Chu B, Zhou JJ, Jamiolkowski DD, Muse E, Dormier E. Macromolecules 1999;32:8107.
[19] Chu B, Harney PJ, Li Y, Yeh F, Hsiao BS. Rev Sci Instrum 1994;65:597.
[20] Song HH, Wu DQ, Chu B, Satkowski M, Stein RS, Phillips JC. Macromolecules 1990;23:2380.
[21] Zhou JJ, Samon JM, Dormier E. J Appl Med Polym 1999;3:55.
[22] Chantani Y, Suehiro K, Okita Y, Tadokoro H, Chujo K. Makromol Chem 1968;113:215.
[23] Strobl GR, Schnieder MJ. J Polym Sci, Polym Phys Ed 1981;19:1361.
[24] Verma R, Marand H, Hsiao B. Macromolecules 1996;29:7767.
[25] Hsiao BS, Wang ZG, Yeh F, Gao Y, Sheth KC. Polymer 1999;40:3515.
[26] Wang ZG, Hsiao BS, Sauer BB, Kampert WG. Polymer 1999;40:4615.
[27] Wang ZG, Hsiao BS, Murthy NS. J Appl Cryst 2000;33:690.
[28] Wang ZG, Hsiao BS, Fu BX, Liu L, Yeh F, Sauer BB, Chang H, Schultz JM. Polymer 2000;41:1791.
[29] Wang ZG, Hsiao BS, Sirota EB, Agarwal P, Srinivas S. Macromolecules 2000;33:978.
[30] Andjelic S, Jamiolkowski D, McDivitt J, Fischer J, Zhou J, Wang ZG, Hsiao BS. J Polym Sci, Polym Phys 2001;1:153.
[31] Wang ZG, Hsiao BS, Lopez J, Armistead JP. J Polym Res — Taiwan 1999;6:167.
[32] Fougnies C, Damman P, Villers D, Dosiere M, Koch MHJ. Macromolecules 1997;30:1385.
[33] Fougnies C, Damman P, Dosiere M, Koch MHJ. Macromolecules 1997;30:1392.
[34] Poussin L, Bertin YA, Parisot J, Brassy C. Polymer 1998;39:4261.
[35] Cheng SZD, Janimak JJ, Zhang A, Hsieh ET. Polymer 1991;32:648.